

Pulse trains propagating through excitable media subjected to external noise

V. Beato^{1,2,a}, H. Engel², and L. Schimansky-Geier³

¹ Technische Universität Berlin, Institut für Theoretische Physik, Hardenbergstr. 36, 10623, Berlin, Germany

² Università “La Sapienza” di Roma, P.le Aldo Moro 2, 00185 Roma, Italy

³ Humboldt-Universität zu Berlin, Institut für Physik, Invalidenstr. 110, 10115 Berlin, Germany

Received 9 January 2007 / Received in final form 17 July 2007

Published online 8 September 2007 – © EDP Sciences, Società Italiana di Fisica, Springer-Verlag 2007

Abstract. We study the propagation of periodic pulse trains in excitable media exposed to external spatio-temporal noise using the light-sensitive Belousov-Zhabotinsky reaction with the underlying Oregonator model as representative example. In the weak noise approximation we find noise-induced transitions in the dispersion relation of pulse trains. We discuss noise-enhanced propagation of pulse trains within a certain wave-length range caused by external noise of moderate strength.

PACS. 05.40.-a Fluctuation phenomena, random processes, noise, and Brownian motion – 82.40.Bj Oscillations, chaos, and bifurcations – 47.54.-r Pattern selection; pattern formation

1 Introduction

The propagation of waves in spatially extended excitable systems is certainly one of the most fascinating examples of self-organization in macroscopic systems far from thermal equilibrium [13,16,32]. Examples include chemical waves in the well-known Belousov-Zhabotinsky reaction (BZ) [45,47], in electro-chemical systems [28] or emerging during catalytic surface reactions [26]. Especially important are excitation waves in biology, where they are widely observed as traveling action potentials in neural and cardiac tissue [14,24], as intra-cellular calcium waves [18,30], and as cAMP waves in aggregating *Dictyostelium* amoebae colonies [42].

Within the macroscopic description of excitable media based on deterministic reaction-diffusion models, internal (thermodynamic) fluctuations are usually neglected (for an example, where internal fluctuations are inherently non-negligible, see [18]). On the other hand, noise effects related to externally imposed fluctuations have been attracting much attention recently. Research in this direction is embedded in the rapidly growing field of noise-induced phenomena in spatially extended non-equilibrium systems [23]. Stochastic resonance [22], spatio-temporal structures induced or stabilized by noise [12,35], and enhanced synchronization of oscillations in the presence of noise are well-known examples. In excitable systems, noise effects include, among others, noise-induced oscillations [17] and coherence resonance [34] (for a comprehensive review see [31]).

One-dimensional spatially extended media support excitation waves of two main types: solitary pulses and periodic pulse trains. Under deterministic, stationary and spatially homogeneous conditions the profile and the speed of a solitary pulse are uniquely determined by the properties of the medium. Because of the existence of a refractory tail behind a pulse, the propagation speed for periodic pulse trains depends on the wavelength. This dependence, called dispersion relation, is one of the basic characteristic of a pulse train. In two spatial dimensions, rotating excitation waves and target patterns can be supported by the medium; none of them are taken into consideration in this work. We emphasize, however, that also for these two-dimensional excitation waves, besides curvature, the dispersion is the defining property.

Recently different noise-induced phenomena have been demonstrated experimentally in the light-sensitive BZ system varying the intensity of applied illumination stochastically in space and time: Noise-supported wave propagation [27], Brownian motion of spiral waves [41], creation of pacemakers out of noise [4], and coherence resonance with respect to the correlation time of colored noise [8].

Even though much has been done theoretically for fronts propagating in uncorrelated fluctuating media [6,33,38–40,48], not much has been predicted in the case of fronts and solitary pulses under the effect of correlated external fluctuations [3,37]. In this paper we concentrate ourselves on pulse trains studying numerically their propagation properties under the influence of external noise. For this purpose we consider the Oregonator model for the light-sensitive variant of the BZ reaction as a representative example of excitable dynamics.

^a e-mail: valentina.beato@roma1.infn.it

The present work is structured as follows: in Section 2 we give a brief introduction of solitary and periodic pulses in the Oregonator model and we introduce the properties of the spatio-temporal stochastic illumination applied to the system. In Section 3 we consider a weak noise expansion for the two-component Oregonator model and we study this issue using a continuation software. Here we discuss noise-induced transitions in the dispersion of pulse trains. We find that fluctuations become important close to a bifurcation in the deterministic system and shift the deterministic threshold. In Section 4, through direct numerical simulations, we show that far from deterministic thresholds noise of moderate intensity can enhance the propagation speed of pulse trains. Section 5 provides a discussion and a short summary.

2 Oregonator model with fluctuating light-intensity

Under deterministic conditions, the kinetic part of the modified Oregonator model for the light-sensitive BZ reaction is given by the following equations for the local concentrations of bromous acid, u , the oxidized form of the catalyst, v , and bromide, w

$$\begin{aligned}\epsilon \frac{du}{dt} &= u - u^2 - w \cdot (u - q) \\ \frac{dv}{dt} &= u - v \\ \epsilon' \frac{dw}{dt} &= fv - w \cdot (u + q) + \phi.\end{aligned}\quad (1)$$

Equation (1) are based on the Tyson-Fife reduction [43] of the Oregonator model for the BZ reaction [20]. Later the model was modified to account for the light-sensitivity of the complex Ruthenium(II)-bipyridyl which now is frequently used as catalyst for the BZ reaction [29]. Today, this model is widely accepted to describe pattern formation in light-sensitive BZ systems.

In equations (1) ϵ , ϵ' , and q are scaling parameters [44], and f is a stoichiometry parameter [11]. The parameter ϕ represents the photochemically induced bromide flow which is assumed to be proportional to the applied light intensity. If for the recipe-dependent internal time scales the relation $1/\epsilon \ll 1/\epsilon'$ holds, the fast variable w can be adiabatically eliminated yielding the two-component version of the Oregonator kinetics

$$\begin{aligned}\epsilon \frac{du}{dt} &= u - u^2 - (fv + \phi) \cdot \frac{u - q}{u + q} \\ \frac{dv}{dt} &= u - v.\end{aligned}\quad (2)$$

If all parameters except the photochemically induced bromide flow ϕ are fixed, then ϕ controls the kinetics and the local excitation threshold. For sufficiently small ϕ -values the kinetics is oscillatory, the system presents an unstable fixed point and a stable limit cycle, as shown by the bifurcation diagram in Figure 1. If we increase ϕ ,

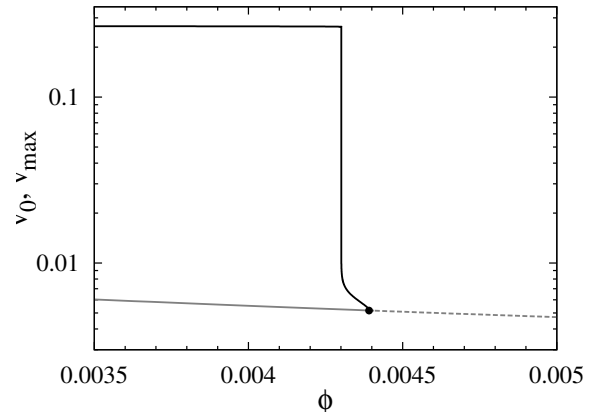


Fig. 1. Bifurcation diagram of the Oregonator kinetics. Black curve: Amplitude of the oscillations measured by the maximal value v_{max} assumed by the inhibitor concentration during a period. Gray curve: value of the inhibitor at unique fixed point v_0 . Full lines denote stable, dashed lines unstable states. Throughout the paper we keep the kinetic parameters fixed: $\epsilon = 0.08525$, $q = 0.002$, and $f = 1.4$.

the system undergoes a super-critical Hopf bifurcation, $\phi_{hb} = 0.00416$, the fixed point becomes stable and the kinetics becomes excitable.

In the case of spatially extended media equations (2) have to be supplemented by diffusion terms describing spatial coupling. In most experiments with the light-sensitive BZ reaction the catalyst is immobilized in a thin gel layer, thus we consider no diffusion for the variable v . This gives

$$\begin{aligned}\frac{\partial u}{\partial t} &= \frac{1}{\epsilon} \left[u - u^2 - (fv + \phi) \cdot \frac{u - q}{u + q} \right] + D_u \nabla^2 u \\ \frac{\partial v}{\partial t} &= u - v,\end{aligned}\quad (3)$$

where ∇^2 denotes the Laplace operator.

Concentration profiles of a typical periodic pulse-train solution obtained in the excitable kinetic regime are shown in Figure 2. The propagation velocity of the pulse depends on the applied illumination via the excitability parameter ϕ . This dependence is plotted in Figure 3. The upper (lower) branch corresponds to stable (unstable) pulse solutions. When the intensity of applied illumination becomes larger, ϕ increases and the pulse moves slower. Beyond the value ϕ_{ext} where both branches merge, the pulse propagation becomes impossible.

Traveling periodic pulse trains are characterized by a dispersion curve which expresses their propagation speed, c , as a function of their wave length, L . The slope of the dispersion curve defines whether the interaction between pulses is attractive (positive slope) or repulsive (negative slope). In the simplest case of so-called normal dispersion $c(L)$ is a monotonously increasing function that approaches the velocity of a solitary pulse c_∞ as $L \rightarrow \infty$. Due to the refractory tail behind excitation leading edge pulse trains are stable only as their wavelength exceeds some minimal value. The BZ reaction shows essentially

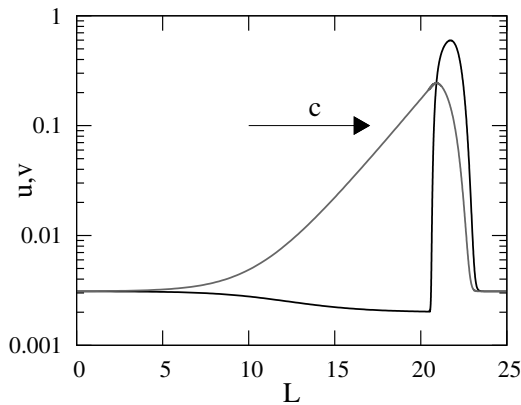


Fig. 2. Activator (black curve) and inhibitor (gray curve) profiles of typical pulse solution of the two-component Oregonator model (Eqs. (3)) in the excitable kinetic regime ($\phi = 0.01$) with diffusion coefficient $D_u = 1$. Numerical simulations were performed in a one-dimensional domain of size $L = 50$ applying periodic boundary conditions. The propagation speed is $c = 4.648$.

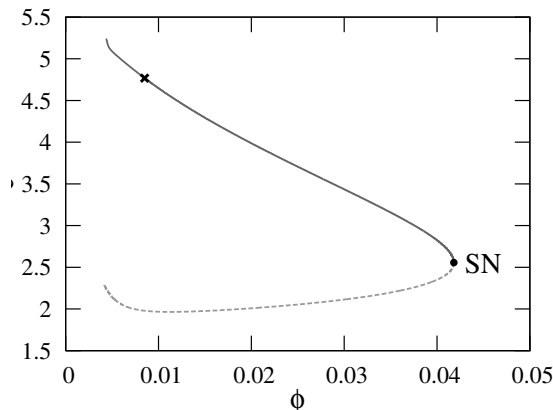


Fig. 3. Propagation velocity c of a periodic pulse-train solution of equations (3) versus the excitability parameter ϕ , wave-length $L = 50$ [1]. The solid line indicates the stable solutions branch, the dashed line the unstable one. The black dot marks the saddle-node bifurcation, the cross correspond to the pulse solution shown in Figure 2.

normal dispersion [21]. Anomalous dispersion includes dispersion curves with negative slope [19,25], oscillatory [46] and bistable dispersion [9,10]. In the latter case, bistability of propagation speed at fixed wave length results in the coexistence of two alternative pulse trains having the same wave length but propagating at different velocity through the medium. Figure 4 shows how the shape of the dispersion curve changes with the excitability parameter ϕ .

To summarize, in the absence of noise the Oregonator model shows the spatio-temporal patterns typical for excitable media as propagating solitary pulses and periodic pulse trains.

Let us now consider the stochastic case with external noise entering through the intensity of incident light. Indeed the applied light intensity controls the local excitation threshold via the photochemical release of the inhibitor bromide. We replace the deterministic parameter

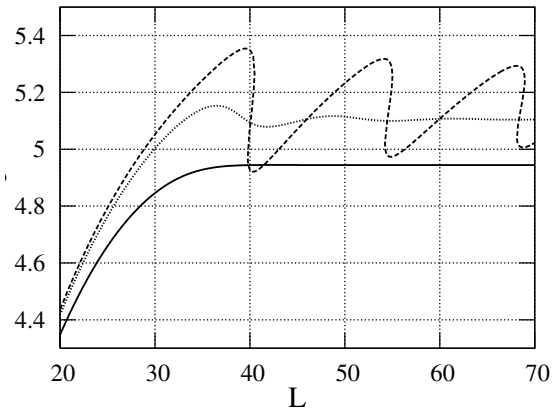


Fig. 4. Dispersion curve for periodic pulse trains at different levels of excitability. Decreasing ϕ from relatively large values, normal dispersion is replaced first by oscillatory and finally by bistable dispersion (solid curve for $\phi = 0.0065$, dotted curve for $\phi = 0.0048$ and dashed curve for $\phi = 0.00433$).

ϕ by the stochastic field

$$\phi \rightarrow \phi(x, t) = \phi_0[1 + \eta(x, t)], \quad (4)$$

where ϕ_0 is proportional to some deterministic reference intensity of applied illumination. Thus in this way we are able to study the pulse propagation in a medium where the excitation threshold varies stochastically in space and time. The stochastic process η is assumed to be Gaussian with zero mean and with a factorized correlation function

$$\Gamma(|x - x'|, |t - t'|) = \gamma_1(|x - x'|)\gamma_2(|t - t'|). \quad (5)$$

The spatial correlation function is triangular, thus

$$\gamma_1(|x - x'|) = \frac{2}{l}(l - |x - x'|)\Theta(l - |x - x'|), \quad (6)$$

where Θ is the Heaviside function and l is proportional to the correlation length λ [2,35,37]. The temporal correlation function is exponentially correlated according to

$$\gamma_2(|t - t'|) = \frac{\sigma^2}{\tau} e^{-|t-t'|/\tau}. \quad (7)$$

Here τ is the correlation time and σ^2 is the intensity of the noise and $\Gamma(0, 0) = \frac{2\sigma^2}{l\tau} = \frac{2\sigma^2}{3\lambda\tau}$.

3 Weak noise expansion

In this section, following an approach put forward by Sancho et al. [36], we derive an effective deterministic equation for the profile and the speed of periodic pulse trains. This approach, which has been successfully extended to various systems and noise signals [3,5,6,23,37], does not correspond to a systematic perturbation expansion in the intensity of the noise. More likely it is based on different time scales of the noise and holds as long as fluctuations of the pulse profile relax much faster than the “wandering of the pulse position” [5].

Our starting point is the two-variable Oregonator model with fluctuating light intensity according to equations (4), (5). It is convenient to rewrite equations (3) as

$$\begin{aligned}\frac{\partial u}{\partial t} &= H(u, v, \eta) + D_u \nabla^2 u \\ \frac{\partial v}{\partial t} &= u - v.\end{aligned}\quad (8)$$

The new reaction term is now given by

$$H(u, v, \eta) = F(u, v) + G(u) \cdot \eta(x, t), \quad (9)$$

for which we have introduced the abbreviations

$$F(u, v) = \frac{1}{\epsilon} \left[u - u^2 - (fv + \phi_0) \cdot \frac{u - q}{u + q} \right], \quad G(u) = \frac{\phi_0}{\epsilon} \frac{u - q}{u + q}. \quad (10)$$

The multiplicative noise term in equation (9) has a non-zero mean value $\langle G(u)\eta(x, t) \rangle \neq 0$. Adding and subtracting this mean value in equation (9), the reaction term can be written as

$$H(u, v, \eta) = F(u, v) + \langle G(u)\eta(x, t) \rangle + R(u, \eta; x, t), \quad (11)$$

where the new random term

$$R(u, \eta; x, t) = G(u) \cdot \eta(x, t) - \langle G(u)\eta(x, t) \rangle \quad (12)$$

has now zero mean, $\langle R(u; x, t) \rangle = 0$. For small and moderate noise intensities it can be neglected in first approximation, $H(u, v, \eta) \simeq F(u, v) + \langle G(u)\eta(x, t) \rangle$. This approximation yields the following statistically equivalent effective deterministic model

$$\begin{aligned}\frac{\partial u}{\partial t} &= F(u, v) + \langle G(u)\eta(x, t) \rangle + D_u \nabla^2 u \\ \frac{\partial v}{\partial t} &= u - v.\end{aligned}\quad (13)$$

To calculate the systematic correction to the reaction function due to noise, i.e. the term $\langle G(u)\eta(x, t) \rangle$, we follow the line of calculations carried out in [37] for the Schlögl model. After straightforward but tedious algebraic transformations we end up with

$$\begin{aligned}\langle G(u)\eta(x, t) \rangle &= \frac{2\sigma^2 \phi_0^2}{3\lambda} \frac{2q}{\epsilon (u + q)^3} \\ &\times \left[(u - q) + \tau \left(\frac{2D_u}{\lambda^2} (q - u) - \frac{4D_u q}{(u + q)^2} \cdot \left(\frac{\partial u}{\partial x} \right)^2 \right. \right. \\ &\left. \left. + \frac{1}{(u + q)} [2qu(u - 1) + u^2 - 2u^3 - q^2(1 - 2u)] \right) \right].\end{aligned}\quad (14)$$

Through its dependence on the noise parameters σ^2 , τ and λ equations (13), (14) determine the way in which spatio-temporal external noise modifies pulse dynamics in the Oregonator model.

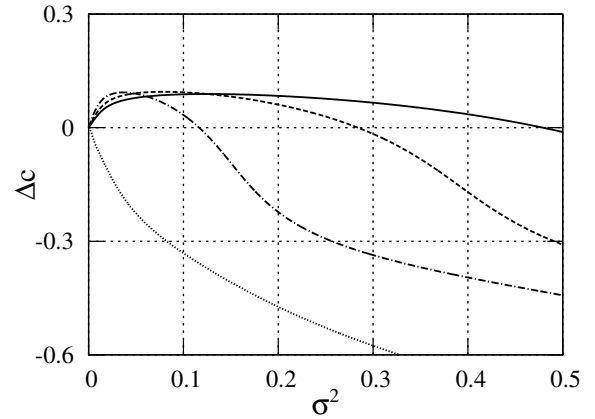


Fig. 5. Speed increment Δc for pulse train solutions with different wavelength at $\phi_0 = 0.0065$. Solid curve for $L = 20$, dashed curve for $L = 22$, dot-dashed curve for $L = 25$ and dotted curve for $L = 40$.

Here, we present results obtained for periodic pulse trains. As mentioned before, we keep the parameters q , f , ϵ and D_u fixed. For the obtained equivalent system of equations (13), (14), a pulse train of wavelength L travels at a speed which depends on the reference illumination ϕ_0 and on the stochastic characteristics of the fluctuating light field. Thus, beyond the dependence on ϕ_0 and L , c turns out to be a function of the noise amplitude σ^2 , the correlation time τ and the correlation length λ . Two-dimensional projections from the high-dimensional parameter space can be generated from the effective deterministic model using the continuation software AUTO [15]. As initial conditions for the continuation analysis we employ a numerical pulse solution of the equations (3) with periodic boundary condition, which is indeed also solution of the system expressed in equations (8) with parameter $\sigma^2 = 0$. We keep here, and further on in this work, $\epsilon = 0.08525$, $f = 1.4$ and $q = 0.002$.

We firstly calculate the branch of solutions of the system of equations (13), (14) in the $c - \sigma^2$ parameter space for $\tau = 0.001$ and $\lambda = 0.015$. These starting values of τ and λ are the typical values of the integration time and space steps, i.e. Δt and Δx , that we adopt for the direct simulations. We plot in Figure 5 the increment of velocity $\Delta c = c_{fluct} - c_{det}$ as a function of the noise intensity. Interestingly this dependence changes qualitatively for solutions of different wavelength.

Of particular interest is the effect of a fluctuating light intensity on the dispersion relation. The calculation of the dispersion curves from the effective deterministic system of equations (13), (14) reveals qualitative changes in the shape of the dependence $c(L)$ as the parameters of the noise are changed. Figure 6 shows a noise-induced transition to a bistable dispersion. This suggests that in a fluctuating medium pulse-trains of same wavelength coexist, which travel at different velocity. In the absence of noise, this kind of transition has been shown for increasing excitability [9], compare Figure 4.

Figure 7 shows that intensity and correlation time of the noise may have a pronounced effect on the propagation

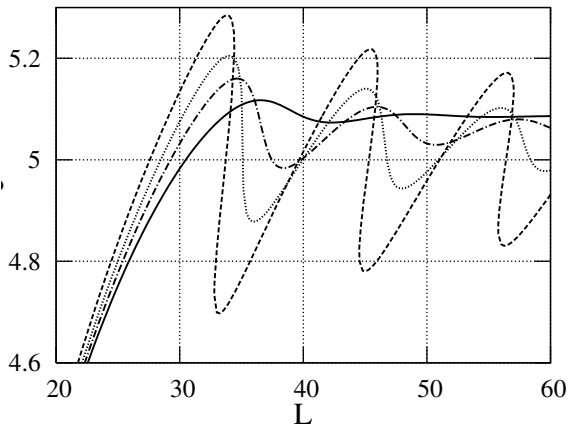


Fig. 6. Emergence of bistability in the dispersion relation for increasing noise intensity, black solid curve for the noiseless case with $\phi_0 = 0.005$. At the same excitability, dot-dashed curve for $\sigma^2 = 0.005$, dotted curve $\sigma^2 = 0.01$, dashed curve $\sigma^2 = 0.02$, value at which the dispersion relation becomes bistable.

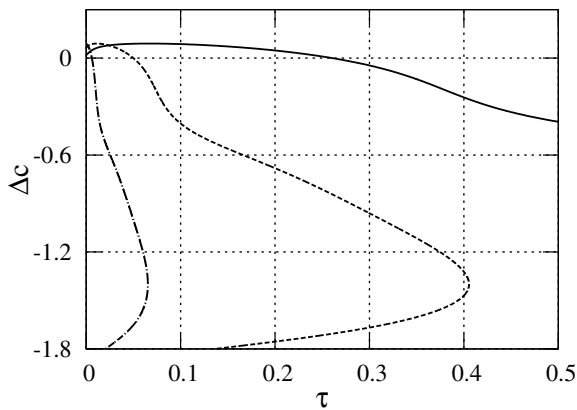


Fig. 7. Noise-induced velocity increments as a function of the correlation time τ for pulse-trains with $\phi_0 = 0.0065$ and wavelength $L = 20$. $\sigma^2 = 0.005$ black curve, $\sigma^2 = 0.025$ dashed curve, $\sigma^2 = 0.5$ dot-dashed curve.

speed of the pulse train. From the same figure we conclude also that in the presence of external noise periodic pulse trains exist only in a certain range of the correlation time below a threshold which depends on σ^2 .

The employed expansion of the correlation $\langle G(u)\eta(x,t) \rangle$ is valid under the assumption of small noise intensity and small correlations. The meaning of small has to be established on the basis of the effects that fluctuations induce on the pulse profiles. The key point of the employed perturbation theory is in fact that the solutions of the effective deterministic system do not deviate significantly from the single stochastic realisations. Santos and Sancho pointed out that spatial correlations can induce distortions in the solutions profile [37]. This turns out to be the case also for pulses in the Oregonator model. Another effect that emerges under spatio-temporally correlated fluctuations is the possible

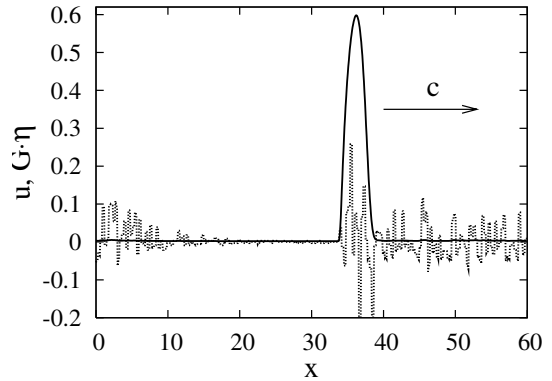


Fig. 8. A snapshot of the activator profile u obtained from direct numerical integration of equations (8) (full line) and a typical realization of the multiplicative noise term $G(u)\eta(x,t)$ enlarged by a factor 2.5×10^3 . The more relevant noise contributions are close to the pulse front and in the rest state of the medium. Noise parameters: $\sigma^2 = 1$, $\tau = 0.5$, and $\lambda = 0.5$.

emergence of new nucleated pulse pairs, events of course not accounted in the present theory.

Summarising, in this section we find different noise-induced effects. Firstly we see that noise can have both a positive and a negative role on the propagation speed of periodic pulse trains: the same noise intensity can increase or decrease the propagation velocity of pulse trains of different wavelength. Moreover we found the emergence under noise of a bistable dispersion relation for periodic pulse-trains.

4 Moderate noise effects

In this section we investigate the effect of fluctuations on the propagation of periodic pulse trains by means of direct numerical simulations. We focus on fluctuations of small and moderate intensity, condition that ensures a well-defined profile for the pulses and thus allows to determine their position and speed. Remarkably, as shown in Figure 8, fluctuations are more relevant in the front of a pulse and in the excited state of the medium, while the refractory region remains almost unaffected by noise.

To study a pulse running along a ring of circumference L , or a periodic pulse train of wavelength L , we integrate equations (3), (4) numerically in a one-dimensional spatial domain of size L adopting periodic boundary conditions. The calculations have been carried out in a co-moving frame which moves at the constant velocity of the pulse train in the absence of noise. We report in Figure 9 a typical space-time plot of the activator variable. Here a pulse that in absence of noise stands at a fixed position (marked with the straight dashed line), starts to move due to the presence of fluctuations in the medium. Therefore numerical simulations reveal a constructive effect of the noise on the pulse propagation. On the other hand, in contrast with the results of Section 4, the reported effect shows up only for fluctuations of moderate intensity, suggesting that this is not a systematic effect. Indeed we find

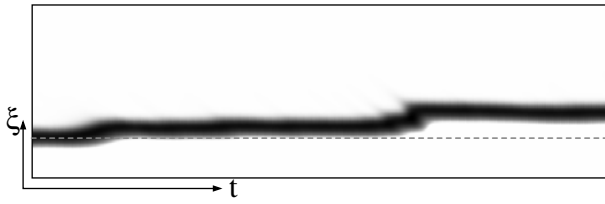


Fig. 9. Space-time plot for the activator variable u traveling in the co-moving frame of coordinate $\xi = x - ct$, with velocity $c = 5.0812$ over a time interval $\Delta T = 25$. System parameters: $\phi_0 = 0.005$, $L = 33.75$. Noise parameters: $\sigma^2 = 0.25$, $\tau = 0.1$, and $\lambda = 0.625$.

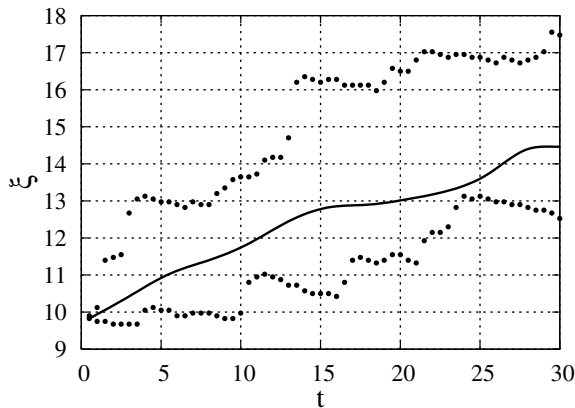


Fig. 10. Space-time plots for pulse trains traveling in the co-moving frame of coordinate $\xi = x - ct$, with velocity $c = 5.0812$. The curves show the trajectories of a detector point placed at the front of the u -profile at a value $u_d = 0.28$. Two different realizations are reported with the dotted curves, the average trajectory, computed over 50 realizations, is shown by the black solid line. System parameters: $\phi_0 = 0.005$, $L = 33.75$. Noise parameters: $\sigma^2 = 0.25$, $\tau = 0.1$, and $\lambda = 1.875$.

that the enhancement of the pulse speed is due to short isolated events (kicks), i.e. when the fluctuations are able to lower the excitation threshold. During these short time intervals the pulse is able to travel faster and to depart from its deterministic straight trajectory.

We track the position of a given point in the front of the pulse and we report in the space-time plot in Figure 10 its mean trajectory (solid line) and two different realizations (dotted lines). The isolated kicks mentioned above manifest in steep increases of the trajectory slope as the pulse crosses a growing super-threshold perturbation. This shows that isolated pulse accelerations induced by noise result in a mean velocity enhancement.

Of course for too small wavelength L the front and the refractory tail of the pulse are close to each other and no noise effects are visible. We emphasize that for pulse trains of small wavelength fluctuations frequently induce super-threshold perturbations in front of the pulse, while nucleation of counter-propagating pulse-pairs from the rest state far from the propagating pulse is almost never observed [7]. Moreover in the case of too large values of L the phenomenon of nucleation can occur, hiding any positive effect of the noise on the pulse propagation. Indeed nucle-

ation events would destroy the analyzed travelling pulse making impossible the study of its propagation properties. Therefore, their absence provides the criterion for an appropriate choice of the noise parameters and the values of ϕ_0 and L . At fixed values of the noise intensity, of the excitation level and of the wavelength, we find that the noise-induced speed enhancement increases with increasing values of the correlation length [7].

5 Conclusions

Due to the possibility to control the local excitation threshold by the intensity of applied illumination light-sensitive BZ media offer broad opportunities for the study of noise-induced phenomena in excitable media. Using a stochastic variant of the modified Oregonator model for the BZ reaction we analyzed the effect of externally imposed fluctuations in the light intensity on the propagation of periodic pulse trains. In the presence of fluctuations the propagation speed depends not only on the excitability parameter ϕ_0 and the wavelength, but also on the characteristics of the noise, i.e., its amplitude, correlation time, and correlation length.

Within the weak noise approximation we demonstrate that the noise intensity and the correlation time have both an effect on the propagation speed and the range of existence of periodic pulse trains. Moreover we find a noise-induced transition from normal to anomalous (bistable) dispersion of pulse trains. This transition can be viewed as an example where fluctuations become important close to a bifurcation in the deterministic system and shift the deterministic threshold.

Beyond the weak noise approximation, when the amplitude of the noise is limited only by the requirement to retain the basic pulse profile and to be unable to nucleate pulse pairs out of the rest state, far from deterministic thresholds noise of moderate intensity can enhance the propagation speed of pulse trains in a certain range of the wavelength. The speed enhancement is due to a small sensibility of the medium to noise in the refractory phase. While fluctuations promote pulse propagation lowering the excitation threshold ahead the pulse, in the refractory tail, where the medium recovers excitability, the deterministic local dynamics is dominant inhibiting noise effects.

A deep understanding of which are the relevant time and length scales of the system in the phenomenon of noise-induced speed enhancement is still poorly understood and remains subject of future research.

References

1. The data presented in this figure, as all the data reported in Figures 1 and 4 and in Section 3, are obtained with the continuation software AUTO. Here the wavelength is equivalent to the domain size L of the medium in the case of direct numerical simulations under the assumption of periodic boundary conditions

2. Such a correlation function is obtained numerically by dividing the spatial domain of size L into m cells of equal size $l = L/m = n\Delta x$, where Δx is the lattice spacing equal to L/N . In each cell ϕ fluctuates homogeneously according to $\phi(x, t) = \phi_0[1 + \eta_i(t)]$ for $il \leq x < (i + 1)l$, where the stochastic variable η_i is a temporally exponentially correlated stochastic process. The correlation length is in this case $\lambda = \frac{n}{3}\Delta x$
3. S. Alonso, F. Sagués, J.M. Sancho, Phys. Rev. E **65**, 066107 (2002)
4. S. Alonso, I. Sendiña-Nadal, V. Pérez-Muñuzuri, J.M. Sancho, F. Sagués, Phys. Rev. Lett. **87**, 078302 (2001)
5. J. Armero, J. Casademunt, L. Ramírez-Piscina, J.M. Sancho, Phys. Rev. E **58**, 5494 (1998)
6. J. Armero, J.M. Sancho, J. Casademunt, A.M. Lacasta, L. Ramírez-Piscina, F. Sagués, Phys. Rev. Lett. **76**, 3045 (1996)
7. V. Beato, *Noise-induced effects in excitable media*, Ph.D. thesis, Technische Universität Berlin, 2005
8. V. Beato, I. Sendiña-Nadal, I. Gerdes, H. Engel, Phys. Rev. E **71**, 035204(R) (2005)
9. G. Bordiougov, H. Engel, Phys. Rev. Lett. **90**, 148302 (2003)
10. G. Bordiougov, H. Engel, Physica D **215**, 25 (2006)
11. H. Brandtstädter, M. Braune, I. Schebesch, H. Engel, Chem. Phys. Lett. **323**, 145 (2000)
12. O. Carrillo, M.A. Santos, J. Garcia-Ojalvo, J.M. Sancho, Europhys. Lett. **65**, 452 (2004)
13. M. Cross, P. Hohenberg, Rev. Mod. Phys. **65**, 851 (1997)
14. J. Davidenko, A. Pertsov, R. Salomonsz, W. Baxter, J. Jalife, Nature **355**, 349 (1992)
15. E.J. Doedel, A.R. Champneys, T.F. Fairgrieve, Y.A. Kuznetsov, B. Sandstede, X.-J. Wang, AUTO97: Continuation and bifurcation software for ordinary differential equations. Technical report, Department of Computer Science, Concordia University, Montreal, Canada, 1997, available by FTP from [ftp.cs.concordia.ca](ftp://ftp.cs.concordia.ca) in directory `pub/doedel/auto`
16. W. Ebeling, *Strukturbildung bei irreversiblen Prozessen* (Teubner-Verlag, Leipzig, 1976)
17. W. Ebeling, H. Herzel, W. Richert, L. Schimansky-Geier, ZAMM **66**, 141 (1986)
18. M. Falcke, Adv. Phys. **53**, 255 (2004)
19. M. Falcke, M. Or-Guil, M. Bär, Phys. Rev. Lett. **84**, 4753 (2000)
20. R. Field, R. Noyes, J. Chem. Phys. **60**, 1877 (1974)
21. J.-M. Flesselles, A. Belmonte, V. Gaspar. J. Chem. Soc., Faraday Trans. **94**, 851 (1998)
22. L. Gammaitoni, P. Hänggi, P. Jung, F. Marchesoni, Rev. Mod. Phys. **70**, 223 (1998)
23. J. García-Ojalvo, J.M. Sancho, *Noise in Spatially Extended Systems* (Springer-Verlag, Berlin, 1999)
24. N. Gorelova, J. Bures, J. Neurobiol **14**, 353 (1983)
25. C.T. Hamik, N. Manz, O. Steinbock, J. Phys. Chem. **105**, 6144 (2001)
26. S. Jakubith, H.H. Rotermund, W. Engel, A. von Oertzen, G. Ertl, PRL **65**, 3013 (1990)
27. S. Kádár, J. Wang, K. Showalter, Nature **391**, 770 (1998)
28. K. Krischer, *Nonlinear dynamics in electrochemical systems*, edited by R. Alkire, D. Kolb, editors, Adv. Electrochem. Sci. Engr. **8**, 89 (2003)
29. H.J. Krug, L. Pohlmann, L. Kuhnert, J. Phys. Chem. **94**, 4862 (1990)
30. J. Lechleiter, S. Girard, E. Peralta, D. Clapham, Science **252**, 123 (1991)
31. B. Lindner, J. García-Ojalvo, A. Neiman, L. Schimansky-Geier, Phys. Reports **392**, 321 (2004)
32. E. Meron, Physics Reports **218**, 1 (1992)
33. A.S. Mikhailov, L. Schimansky-Geier, W. Ebeling, Phys. Lett. A **96**, 453 (1983)
34. A.S. Pikovsky, J. Kurths, Phys. Rev. Lett. **78**, 775 (1997)
35. X. Sailer, D. Hennig, V. Beato, H. Engel, L. Schimansky-Geier, Phys. Rev. E **73**, 056209 (2006)
36. J.M. Sancho, M.S. Miguel, S.L. Katz, J.D. Gunton, Phys. Rev. A **26**, 1589 (1982)
37. M.A. Santos, J.M. Sancho, Phys. Rev. E **64**, 016129 (2001)
38. M.A. Santos, C.Zülicke, L. Schimansky-Geier, Phys. Lett. A **290**, 270 (2001)
39. L. Schimansky-Geier, A.S. Mikhailov, W. Ebeling, Ann. der Phys. **40**, 277 (1983)
40. L. Schimansky-Geier, C. Zülicke, Z. Phys. B **82**, 157 (1991)
41. I. Sendiña-Nadal, S. Alonso, V. Pérez-Muñuzuri, M.Gómez-Gesteira, V. Pérez-Villar, L. Ramírez-Piscina, J. Casademunt, J.M. Sancho, F. Sagués, Phys. Rev. Lett. **84**, 2734 (2000)
42. F. Siegert, C. Weijer, Proc. Natl. Acad. Sci. USA **89**, 6433 (1992)
43. J. Tyson, P. Fife, J. Chem. Phys. **73**, 2224 (1980)
44. J.J. Tyson, P. Fife, J. Chem. Phys. **73**, 2224 (1980)
45. A. Winfree, Science **175**, 634 (1972)
46. A.T. Winfree, Physica D **49**, 125 (1991)
47. A. Zaikin, A. Zhabotinsky, Nature **225**, 535 (1970)
48. C.Zülicke, A.S. Mikhailov, L. Schimansky Geier, Physica A **163**, 559 (1990)